Polarization transfer in the $^2\mathrm{H}(\vec{e}, e'\vec{p})n$ reaction up to $Q^2 = 1.61$ (GeV/c)^2

B. Hu,[1] M. K. Jones,[2] P. E. Ulmer,[2] H. Arenhövel,[3] O. K. Baker,[1] W. Bertozzi,[4] E. J. Brash,[5] J. Calarco,[6] J.-P. Chen,[7] E. Chudakov,[7] A. Cochran,[1] S. Dumalski,[5] R. Ent,[1,7] J. M. Finn,[8] F. Garibaldi,[9] S. Gilad,[4] R. Gilman,[7,10] C. Glashausser,[10] J. Gomez,[7] V. Gorbenko,[11] J.-O. Hansen,[7] J. Hovebo,[5] C. W. de Jager,[7] S. Jeschonnek,[12] X. Jiang,[10] C. Keppel,[1] A. Klein,[2] A. Kozlov,[5] S. Kuhn,[2] G. Kumbartzki,[10] M. Kuss,[7] J. J. LeRose,[7] M. Liang,[7] N. Liyanage,[4] G. J. Lolos,[5] P. E. C. Markowitz,[13] D. Meekins,[14] R. Michaels,[7] J. Mitchell,[7] Z. Papandreou,[15] C. F. Perdrisat,[8] V. Punjabi,[16] R. Roche,[14] D. Rowntree,[4] A. Saha,[7] S. Strauch,[10] L. Todor,[2] G. Urciuoli,[9] L. B. Weinstein,[2] K. Wijesooriya,[8] B. B. Wojtsekhowski,[7] and R. Woo[17]

[1]*Hampton University, Hampton, Virginia 23668, USA*
[2]*Old Dominion University, Norfolk, Virginia 23529, USA*
[3]*Johannes Gutenberg-Universität, D-55099 Mainz, Germany*
[4]*Massachusetts Institute of Technology, Cambridge, Massachusetts 02139, USA*
[5]*University of Regina, Regina, SK, Canada S4S 0A2, CANADA*
[6]*University of New Hampshire, Durham, New Hampshire 03824, USA*
[7]*Thomas Jefferson National Accelerator Facility, Newport News, Virginia 23606, USA*
[8]*College of William and Mary, Williamsburg, Virginia 23187, USA*
[9]*INFN, Sezione Sanitá and Istituto Superiore di Sanitá, Laboratorio di Fisica, I-00161 Rome, Italy*
[10]*Rutgers, The State University of New Jersey, Piscataway, New Jersey 08855, USA*
[11]*Kharkov Institute of Physics and Technology, Kharkov 310108, Ukraine*
[12]*The Ohio State University, Lima, Ohio 45804, USA*
[13]*Florida International University, Miami, Florida 33199, USA*
[14]*Florida State University, Tallahassee, Florida 32306, USA*
[15]*The George Washington University, Washington, DC 20052, USA*
[16]*Norfolk State University, Norfolk, Virginia 23504, USA*
[17]*TRIUMF, Vancouver, British Columbia, Canada V6T 2A3, CANADA*

(Received 18 January 2006; published 27 June 2006)

The recoil proton polarization was measured in the $^2\mathrm{H}(\vec{e}, e'\vec{p})n$ reaction in Hall A of the Thomas Jefferson National Accelerator Facility. The electron kinematics were centered on the quasielastic peak ($x_{Bj} \approx 1$) and included three values of the squared four-momentum transfer, $Q^2 = 0.43$, 1.00 and 1.61 (GeV/c)^2. For $Q^2 = 0.43$ and 1.61 (GeV/c)^2, the missing momentum, p_m, was centered at zero, whereas for $Q^2 = 1.00$ (GeV/c)^2 two values of p_m were chosen: 0 and 174 MeV/c. At low p_m, the Q^2 dependence of the longitudinal polarization, P'_z, is not well described by a state-of-the-art calculation. Further, at higher p_m, a 3.5σ discrepancy was observed in the transverse polarization, P'_x. Understanding the origin of these discrepancies is important to confidently extract the neutron electric form factor from the analogous $^2\mathrm{H}(\vec{e}, e'\vec{n})p$ experiment.

DOI: 10.1103/PhysRevC.73.064004 PACS number(s): 25.30.Fj, 13.40.Gp, 13.88.+e, 14.20.Dh

I. INTRODUCTION

In the loosely bound deuteron, the proton and neutron are expected to behave essentially as free particles in intermediate energy nuclear reactions with appropriate kinematics. This expectation and the absence of suitable pure neutron targets make the deuteron a natural choice for extracting properties of the neutron. Though the neutron elastic electric form factor has been especially difficult to extract, the use of polarized beams and targets in $^2\vec{\mathrm{H}}(\vec{e}, e'n)p$ [1,2] and polarized beams with neutron recoil polarimetry in $^2\mathrm{H}(\vec{e}, e'\vec{n})p$ [3–7] has allowed statistically precise measurements.

For elastic electron scattering from a free nucleon, it was shown in Refs. [8,9] that the polarizations transferred from a longitudinally polarized electron beam to the recoil nucleon [i.e., via the $(\vec{e}, e'\vec{p}\,)$ or $(\vec{e}, e'\vec{n}\,)$ reaction] can be expressed in terms of the nucleon electromagnetic form factors. This technique has been exploited to measure the proton electric to magnetic form factor ratio for large values of the squared four-momentum transfer, Q^2, using a hydrogen target [10–12]. To extract the neutron electric form factor, the $^2\mathrm{H}(\vec{e}, e'\vec{n})p$ reaction has been exploited at the MIT-Bates Laboratory [3], Mainz [4,5,7], and Jefferson Lab (JLab) [6]. However, nuclear effects can compromise the direct connection between the polarization transfer coefficients and the neutron form factors. This is especially true of the neutron electric form factor, given its small size relative to possible competing effects. It is therefore essential that reaction models be tested experimentally. The present experiment, employing the $^2\mathrm{H}(\vec{e}, e'\vec{p})n$ reaction, provides the means for evaluating the validity of extracting form factors from the polarization transfer coefficients, because the polarization observables can be compared directly with those obtained from a free proton target via the elastic $^1\mathrm{H}(\vec{e}, e'\vec{p}\,)$ reaction. (In addition, our data may provide useful information for the related $^4\mathrm{He}(\vec{e}, e'\vec{p}\,)^3\mathrm{H}$ experiments [13–15], where the higher nuclear density likely leads to more important nuclear effects.)

In the simplest picture of the $^2\mathrm{H}(\vec{e}, e'\vec{p})n$ reaction, the plane-wave impulse approximation (PWIA), the proton is

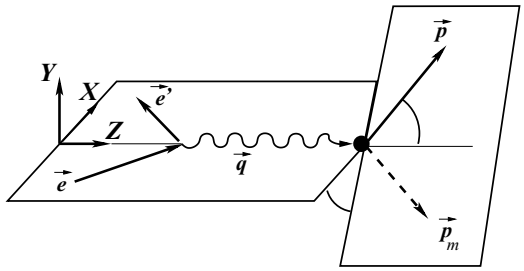

FIG. 1. Coordinate system used to define the polarization components. The Z axis is along the momentum transfer $\vec{q}$, the Y axis is in the direction of $\vec{e} \times \vec{e}\,'$ (where $\vec{e}$ and $\vec{e}\,'$ are the momenta of the incident and scattered electron, respectively) and the X axis is in the electron-scattering plane completing the right-handed system. Here, $\vec{p}$ is the momentum of the recoiling proton and $\vec{p}_m$ is the missing momentum. The "out-of-plane" angle is the angle between the two depicted planes, the scattering plane and the hadronic plane.

knocked out by the virtual photon and is detected without any further interaction with the unobserved neutron. In this picture, the transferred polarizations (see Fig. 1 for an illustration of the coordinate system) along the momentum transfer direction, P'_z, and in the scattering plane, perpendicular to the momentum transfer, P'_x, can be expressed in terms of various kinematical factors and the ratio of the proton electric and magnetic form factors (G_E and G_M, respectively) [16]. Various calculations [17–23] predict that polarizations measured in the $^2\mathrm{H}(\vec{e}, e'\vec{n})p$ and $^2\mathrm{H}(\vec{e}, e'\vec{p})n$ reactions for kinematics close to zero missing momentum (p_m, where $\vec{p}_m \equiv \vec{q} - \vec{p}$ with $\vec{q}$ the three-momentum transfer and $\vec{p}$ the momentum of the detected nucleon) are expected to be nearly free from the effects of interaction currents [meson exchange currents (MEC) and isobar configurations (IC)] as well as final-state interactions (FSI) between the outgoing nucleons. It is precisely the predicted insensitivity to such effects that made the $^2\mathrm{H}(\vec{e}, e'\vec{n})p$ reaction a natural choice for the extraction of the neutron electric form factor. However, the moderate experimental acceptances employed in these experiments entail an average over kinematics outside the ideal limit of $p_m = 0$. Polarizations measured in the $^2\mathrm{H}(\vec{e}, e'\vec{p})n$ reaction can test some of the model assumptions over the kinematical range of interest.

To date only two other experiments on the $^2\mathrm{H}(\vec{e}, e'\vec{p})n$ reaction exist, one performed at the Mainz Microtron (MAMI) facility [24] and the other at the MIT-Bates Laboratory [25]. They were restricted to squared four-momentum transfers of $Q^2 = 0.3(\mathrm{GeV}/c)^2$ (Mainz) and $Q^2 = 0.38$ and $0.50\,(\mathrm{GeV}/c)^2$ (Bates) and also to low p_m. The data from both experiments were well described by theoretical models. The current JLab experiment was able to achieve higher Q^2 and p_m values with smaller statistical uncertainties.

II. EXPERIMENTAL DETAILS

Three of our kinematics settings were centered at $p_m = 0$, roughly covering the Q^2 range of the JLab $^2\mathrm{H}(\vec{e}, e'\vec{n})p$ experiment [6]. At each of these kinematics, both $^2\mathrm{H}(\vec{e}, e'\vec{p})n$ and $^1\mathrm{H}(\vec{e}, e'\vec{p})$ data were acquired. This allowed forming ratios of the polarizations for deuterium and hydrogen targets, providing a measure of nuclear effects. A fourth kinematics was selected at nonzero p_m, at the intermediate Q^2 value, to test reaction models in a region where interaction effects are expected to be somewhat larger. Furthermore, this kinematics is relevant for the $^2\mathrm{H}(\vec{e}, e'\vec{n})p$ experiment given that its acceptance includes p_m values of this magnitude.

TABLE I. Kinematics (central values) for the present experiment. The beam energy was 1.669 GeV for all kinematics.

Q^2 $[(\mathrm{GeV}/c)^2]$	p_m (MeV/c)	Electron momentum (GeV/c)	Electron θ_{LAB} (deg)	Proton momentum (GeV/c)	Proton θ_{LAB} (deg)
0.43	0	1.429	24.45	0.692	−58.97
1.00	0	1.127	42.65	1.128	−42.68
1.61	0	0.804	66.23	1.525	−28.91
1.00	174	1.127	42.65	1.128	−33.88

The experiment was performed in Hall A of JLab using the high-resolution spectrometer pair. The relevant kinematical parameters are given in Table I. Details of the Hall A instrumentation are given elsewhere [26]. Electrons were detected in the "Left" spectrometer, whereas protons were detected in the "Right" spectrometer. The targets consisted of 15-cm-long liquid hydrogen and deuterium cells. The Left spectrometer included an atmospheric pressure CO_2 Cerenkov detector used to reject π^- events. To reduce other backgrounds, nominal cuts were placed on the vertex and angular variables reconstructed at the target. Uncorrelated *ep* coincidences were removed via cuts on the coincidence time-of-flight, as well as cuts on the missing mass and missing momentum. The experiment used beam currents of up to 50 μA combined with a beam polarization of 76%, measured using a Møller polarimeter. The beam helicity was flipped pseudorandomly to reduce systematic uncertainties of the extracted polarization transfer observables. The proton spectrometer was equipped with a focal plane polarimeter (FPP) [12]. Polarized protons scatter azimuthally asymmetrically in the carbon analyzer of the FPP. The analyzer thicknesses employed are given in Table II. To reduce Coulomb scattering for which the analyzing power is identically zero, cuts restricting the polar angle of the second-scattering distribution were enforced and are shown in Table II. The resulting distributions, in combination with information on the beam helicity, were analyzed by means of a maximum likelihood method to obtain the transferred polarization components. More details on the analysis can be found in Refs. [12,27].

TABLE II. Thickness of the FPP graphite analyzer for each of our kinematics. Also shown are the cuts we placed on the polar angle of the second scattering in the FPP.

Q^2 $[(\mathrm{GeV}/c)^2]$	p_m (MeV/c)	Analyzer thickness (inches)	θ_{FPP} cut (deg)
0.43	0	3.0	3–30
1.00	0	9.0	3–30
1.61	0	16.5	3–40
1.00	174	9.0	3–30

TABLE III. The form factor ratio obtained from our ^{1}H($\vec{e}, e'\vec{p}$) data, scaled by the proton magnetic moment, μ. The uncertainties are statistical and systematic respectively.

Q^2 [(GeV/c)^2]	$\mu G_E/G_M$
0.43	$0.994 \pm 0.034 \pm 0.005$
1.00	$0.879 \pm 0.022 \pm 0.013$
1.61	$0.865 \pm 0.039 \pm 0.036$

III. CALIBRATION WITH THE HYDROGEN TARGET

As a check, our ^{1}H($\vec{e}, e'\vec{p}$) data were compared with the extracted G_E/G_M ratio from previous experiments which also used the recoil polarization technique. Our results, listed in Table III and plotted as filled diamonds in Fig. 2, are seen to agree well with previous measurements. Also shown in Fig. 2 is $\mu G_E/G_M$ for the Lomon GKex(02S) form factors [28]. The Lomon form factors agree well with the polarization transfer data in this Q^2 range and were therefore incorporated in our ^{2}H($\vec{e}, e'\vec{p}$)n calculations (see below).

IV. RESULTS AND DISCUSSION

Figure 3 and Table IV show results for the three measurements centered at $p_m = 0$. The top three panels show P'_x, P'_z and P'_x/P'_z compared to the PWIA calculation. The bottom panel shows the double ratio, $(P'_x/P'_z)_D/(P'_x/P'_z)_H$, defined as the ratio P'_x/P'_z for ^{2}H($\vec{e}, e'\vec{p}$)n divided by the same ratio for ^{1}H($\vec{e}, e'\vec{p}$). Only statistical uncertainties are shown in the figure; the systematic uncertainties are given in the table and are discussed in detail later in the article. The calculations shown are from Arenhövel [23]. The plane-wave Born approximation (PWBA) calculation includes scattering from the neutron with

TABLE IV. The polarizations, P'_x and P'_z, and the ratio, P'_x/P'_z, as a function of Q^2 for the ^{2}H($\vec{e}, e'\vec{p}$)n measurements centered at $p_m = 0$. Also shown are the double ratios, defined in the text. The uncertainties are statistical and systematic respectively. For P'_x and P'_z, the statistical uncertainty includes a contribution from the statistical uncertainty in our extraction of the analyzing power, A_c, amounting to $\Delta A_c/A_c = 2.7$, 1.4, and 2.3% for $Q^2 = 0.43$, 1.00, and 1.61, respectively.

Q^2 [(GeV/c)^2]	P'_x	P'_z
0.43	$-0.218 \pm 0.008 \pm 0.0006$	$0.236 \pm 0.008 \pm 0.0009$
1.00	$-0.299 \pm 0.006 \pm 0.003$	$0.557 \pm 0.009 \pm 0.003$
1.61	$-0.279 \pm 0.011 \pm 0.011$	$0.722 \pm 0.024 \pm 0.004$
	P'_x/P'_z	$(P'_x/P'_z)_D/(P'_x/P'_z)_H$
0.43	$-0.924 \pm 0.029 \pm 0.005$	$0.926 \pm 0.044 \pm 0.0005$
1.00	$-0.537 \pm 0.010 \pm 0.008$	$1.001 \pm 0.030 \pm 0.0007$
1.61	$-0.387 \pm 0.015 \pm 0.016$	$1.077 \pm 0.070 \pm 0.0015$

detection of the spectator proton. (As our kinematics involve relatively high momentum transfers and are centered on $p_m = 0$, the PWBA calculation is nearly identical to the PWIA calculation that includes only scattering from the proton.) The distorted-wave Born approximation (DWBA) calculation includes pn final-state rescattering (FSI). The DWBA + MEC + IC calculation includes also non-nucleonic currents (MEC and IC) and the full calculation (DWBA + MEC + IC + RC) further includes relativistic contributions of leading order in p/m to the kinematical wave function boost and to the nucleon current. The Bonn two-body interaction [30] and the Lomon GKex(02S) nucleon form factors [28] were used. The models were acceptance averaged using MCEEP [31] via interpolation over a kinematical grid. The polarizations

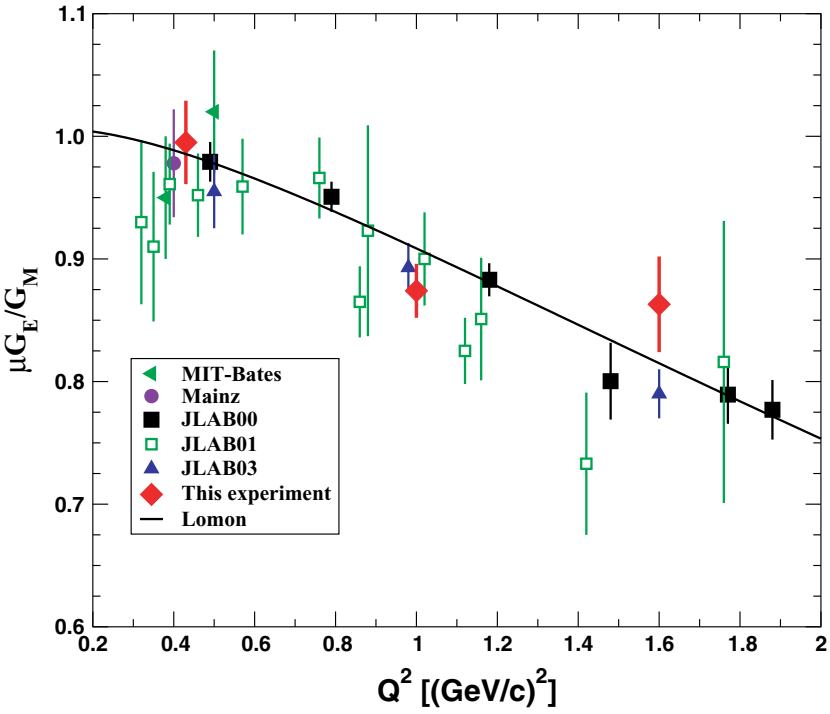

FIG. 2. (Color online) The filled diamonds are $\mu G_E/G_M$ for this experiment. Data from other Jefferson Lab experiments are labeled as JLAB00 [12], JLAB01 [29], and JLAB03 [27]. Data from other laboratories are labeled as MIT-Bates [25] and Mainz [13]. The curve shows $\mu G_E/G_M$ for the Lomon GKex(02S) form factors [28].

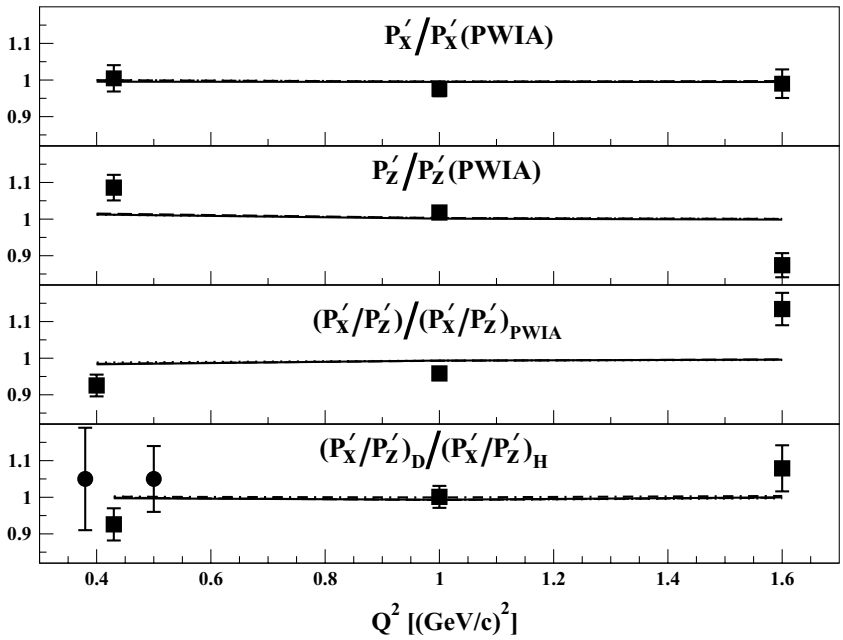

FIG. 3. The open circles are the MIT-Bates data [25] and the solid squares represent the data from the present experiment. The dot-dashed curves are for the plane-wave Born approximation (PWBA), the dotted curves are for the distorted-wave Born approximation (DWBA), the dashed curves include MEC and IC, and the solid curves are the full calculations that also include relativistic corrections (RC). The top two panels show P'_x and P'_z, normalized to the PWIA calculation. The third panel shows P'_x/P'_z compared to the same ratio calculated in PWIA. The bottom panel shows the double ratio, defined in the text.

computed by Arenhövel were rotated from the center-of-mass system into the coordinate system of Fig. 1 within MCEEP. Radiative folding was carried out within the framework of Borie and Drechsel [32]. It can be seen that the predicted nuclear effects are quite small for these kinematics. However, the full calculation does not give the correct Q^2 dependence for P'_z. The χ^2 per degree of freedom of the three P'_z data points relative to the full calculation is 5.9/3, implying a 12% probability that our data are consistent with the theory. Given the somewhat poorer statistical uncertainties, the χ^2 per degree of freedom for the double ratio deviates from the full calculation by 3.9/3, implying a 27% probability of consistency. As can be seen from Fig. 2, our highest Q^2 ^{1}H$(\vec{e}, e'\vec{p})$ datum lies above the world average. Coupled with the relatively larger uncertainty of this datum, the double ratio at this Q^2 agrees better with theory than the single ratio, P'_x/P'_z. It should be cautioned that the lowest Q^2 point is the only one within the proton kinetic energy range used to determine the Bonn potential. Two-photon exchange processes, not included in our calculations, are estimated to have only minor effects on the transferred polarizations in the elastic ^{1}H$(\vec{e}, e'\vec{p})$ reaction [33]. The effects on P'_x and P'_z are estimated to be less than 0.5% for $Q^2 = 1$ over the entire ϵ (longitudinal photon polarization) range. Because our ^{2}H$(\vec{e}, e'\vec{p})n$ kinematics are on the quasifree peak, we expect the effects of two-photon exchange to be of similar size.

In Fig. 4 and Table V the p_m dependence of the polarizations, P'_x and P'_z, as well as the polarization ratio,

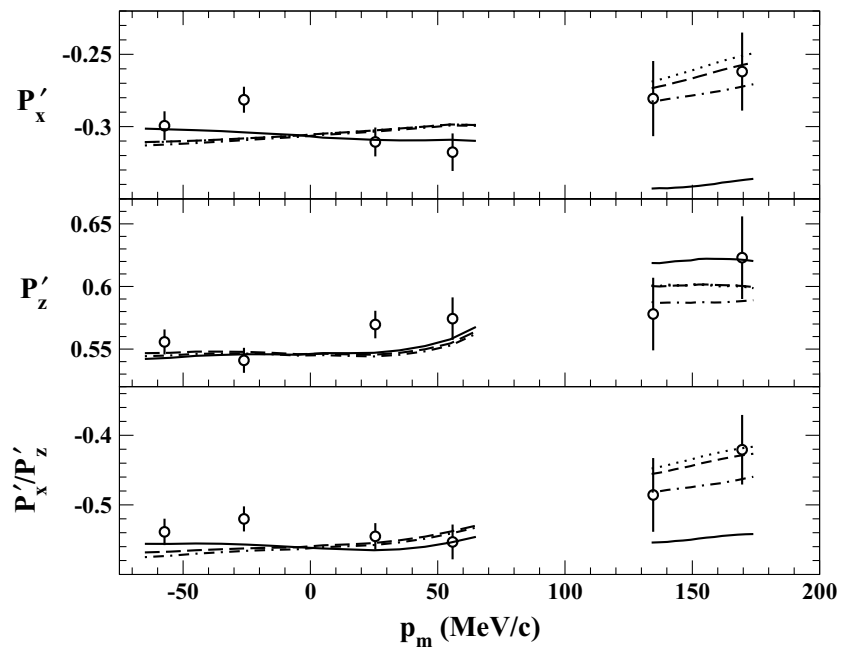

FIG. 4. The polarizations P'_x, P'_z and the ratio P'_x/P'_z as a function of p_m at $Q^2 = 1.00$ (GeV/c)^2. The p_m values shown correspond to cross-section weighted averages. The labeling of the theoretical curves is the same as for the previous figure. At low p_m all curves except for the solid (DWBA + MEC + IC + RC) are essentially indistinguishable. For P'_z at high p_m the dotted (DWBA) and dashed (DWBA + MEC + IC) curves are indistinguishable.

TABLE V. The polarizations P'_x, P'_z and the ratio P'_x/P'_z along with their statistical uncertainties as a function of p_m at $Q^2 = 1.00$ (GeV/c)^2. The statistical uncertainty includes a contribution from the statistical uncertainty in A_c, amounting to 1.35%, except for the highest two p_m points where it is negligible. The systematic uncertainties are essentially independent of p_m and are estimated to be 0.004, 0.002, and 0.008 for P'_x, P'_z, and P'_x/P'_z respectively.

p_m (MeV/c)	P'_x	P'_z	P'_x/P'_z
−57	-0.299 ± 0.010	0.556 ± 0.013	-0.539 ± 0.019
−26	-0.281 ± 0.009	0.541 ± 0.013	-0.520 ± 0.018
26	-0.311 ± 0.010	0.570 ± 0.013	-0.545 ± 0.019
56	-0.318 ± 0.013	0.574 ± 0.017	-0.553 ± 0.025
135	-0.281 ± 0.026	0.578 ± 0.029	-0.485 ± 0.052
170	-0.262 ± 0.027	0.623 ± 0.033	-0.420 ± 0.050

P'_x/P'_z, is shown for $Q^2 = 1.00$(GeV/c)^2. Only the statistical uncertainties are plotted in the figure; the relatively smaller systematic uncertainties are given in the table caption. The group of points at low p_m were obtained by binning the data for the $p_m = 0$ kinematics, whereas the pair of data points at higher p_m were obtained by binning the data for the $p_m = 174$ MeV/c kinematics. The proton spectrometer angles differ between the two kinematics, which gives rise to the discontinuities in the calculations between low and high p_m. At low p_m nuclear effects are predicted to have little influence, consistent with the results shown in Fig. 3. This is expected because the latter represents an average over the four low p_m points in Fig. 4. At high p_m nuclear effects and especially relativistic effects are significantly larger. For P'_z at high p_m, the data and full calculation agree, whereas for P'_x there is a 3.5σ discrepancy, after combining the two highest p_m data points.

The discrepancy observed at our high-p_m kinematics may have serious implications for the ^{2}H($\vec{e}, e'\vec{n}$)p experiment. In fact, because nuclear effects are predicted to be larger for the neutron experiment (comparison between Arenhövel's calculations for the present experiment and for the ^{2}H($\vec{e}, e'\vec{n}$)p experiment [34] suggest that nuclear effects are four to six times larger for the neutron case at the lowest and highest Q^2 kinematics, respectively), one might expect any deviation from the calculation to be larger as well. Without knowledge of the dependence of the discrepancy on p_m and on the out-of-plane angle (see Fig. 1) one cannot quantitatively assess the effect on the neutron experiment. However, under certain assumptions, one can make an estimate. To this end, we assume that the discrepancy is proportional to p_m (and therefore zero at $p_m = 0$) and has no dependence on the out-of-plane angle. In this case, our discrepancy would imply a (6±2)% effect on the neutron form factor at the intermediate Q^2, where we have weighted over the acceptance of the neutron experiment. This assumes that there is no magnification in the effect between the ^{2}H($\vec{e}, e'\vec{p}$)n and ^{2}H($\vec{e}, e'\vec{n}$)p experiments. If, however, we use the ratio of nuclear effects within the model of Arenhövel as a guide, the effect on the neutron form factor increases to (27±8)%. We caution that these estimates involve a host of assumptions. Only additional data can answer the question definitively.

TABLE VI. The breakdown of systematic uncertainties for each kinematics. The values shown represent absolute uncertainties on the various quantities. Here $\theta_{\rm bend}$ and $\phi_{\rm bend}$ refer to the uncertainties arising from imperfect knowledge of the dispersive and nondispersive bend angles in the spectrometer, respectively, whereas $\phi_{\rm FPP}$ denotes the uncertainty from the azimuthal angle in the FPP. The $\theta_{\rm bend}$ contribution to the uncertainty in P'_x is dominated by the uncertainty in our extraction of the analyzing power (see the text for details). The "Total" uncertainty is the quadrature sum of the various contributions. Note that, because of correlations, the uncertainty in P'_x/P'_z is not simply the quadrature sum of the uncertainties in P'_x and P'_z.

$Q^2 = 0.43$ [(GeV/c)^2] $p_m = 0$ MeV/c	P'_x	P'_z	P'_x/P'_z	$(P'_x/P'_z)_D/(P'_x/P'_z)_H$
$\theta_{\rm bend}$	0.00000	0.00070	0.0029	0.00005
$\phi_{\rm bend}$	0.00015	0.00015	0.0015	0.00045
$\phi_{\rm FPP}$	0.00050	0.00050	0.0037	0.00000
Total	0.00056	0.00087	0.0050	0.00045
$Q^2 = 1.00$ [(GeV/c)^2] $p_m = 0$ MeV/c	P'_x	P'_z	P'_x/P'_z	$(P'_x/P'_z)_D/(P'_x/P'_z)_H$
$\theta_{\rm bend}$	0.0029	0.0027	0.0074	0.00006
$\phi_{\rm bend}$	0.0005	0.0003	0.0012	0.00064
$\phi_{\rm FPP}$	0.0009	0.0007	0.0024	0.00018
Total	0.0031	0.0028	0.0079	0.00067
$Q^2 = 1.61$ [(GeV/c)^2] $p_m = 0$ MeV/c	P'_x	P'_z	P'_x/P'_z	$(P'_x/P'_z)_D/(P'_x/P'_z)_H$
$\theta_{\rm bend}$	0.011	0.0040	0.016	0.0014
$\phi_{\rm bend}$	0.001	0.0002	0.001	0.0006
$\phi_{\rm FPP}$	0.001	0.0011	0.002	0.0000
Total	0.011	0.0042	0.016	0.0015
$Q^2 = 1.00$ [(GeV/c)^2] $p_m = 174$ MeV/c	P'_x	P'_z	P'_x/P'_z	
$\theta_{\rm bend}$	0.0038	0.0019	0.0071	
$\phi_{\rm bend}$	0.0007	0.0002	0.0023	
$\phi_{\rm FPP}$	0.0011	0.0007	0.0023	
Total	0.0040	0.0020	0.0078	

V. SYSTEMATIC UNCERTAINTIES

The breakdown of the systematic uncertainties for P'_x, P'_z, P'_x/P'_z, and $(P'_x/P'_z)_D/(P'_x/P'_z)_H$ is given in Table VI. The uncertainties are dominated by uncertainty in the precession of the proton's spin in the spectrometer magnetic fields. The spin precession is characterized by a rotation matrix that relates the polarizations measured with the FPP to the polarizations at the experimental target, P'_x and P'_z. The matrix was obtained using the COSY [35] transport program applied to the magnetic elements of the Hall A "Right" spectrometer. Although COSY employs a differential algebraic method to calculate the transfer matrix, the spin matrix can also be

calculated using a geometric model [12]. In the latter approach the elements of the spin matrix are based on the proton's bend angles in the spectrometer. Because the uncertainties in the bend angle can be measured, this approach facilitates estimation of the precession-related systematic uncertainties. So, although COSY was used to extract the target polarizations from those measured at the FPP, the geometric model was employed to estimate our systematic uncertainties. To improve the knowledge of systematics for the general program of Hall A recoil polarization experiments, two dedicated experiments were conducted to determine the magnitude of the bend angle in the nondispersive plane along with its uncertainty. The uncertainty of the bend angle in the dispersive plane was measured independently during the experiment of Ref. [12]. The geometric model was then used to estimate the resulting systematic uncertainties on P'_x and P'_z (the systematic uncertainties on P'_x and P'_z are dominated by uncertainties in the bend angle in the nondispersive and dispersive planes, respectively). For the double ratio, $(P'_x/P'_z)_D/(P'_x/P'_z)_H$, the systematic uncertainty almost completely cancels because the outgoing protons from both reactions travel through essentially the same magnetic fields. Finally, especially for the lowest Q^2 measurement, uncertainty in knowledge of the azimuthal angle of the proton in the FPP makes a significant contribution to the overall systematic uncertainty.

For $^1\mathrm{H}(\vec{e}, e'\vec{p})$, both P'_x and P'_z depend on the product hA_c (where h is the beam polarization and A_c is the analyzing power of the FPP) and the proton form factor ratio, G_E/G_M. Therefore, measurement of both polarization components in $^1\mathrm{H}(\vec{e}, e'\vec{p})$ allows determination of G_E/G_M and the product hA_c. The analyzing power can then be determined because h is measured independently with the Møller polarimeter. Note that an uncertainty in h induces an uncertainty in A_c. However, assuming that h does not change between the consecutive $^1\mathrm{H}(\vec{e}, e'\vec{p})$ and $^2\mathrm{H}(\vec{e}, e'\vec{p})n$ measurements, any uncertainty in this quantity will completely cancel against the induced uncertainty in A_c in our extraction of P'_x and P'_z for the $^2\mathrm{H}(\vec{e}, e'\vec{p})n$ measurement. Our extraction of A_c is mostly sensitive to the uncertainty in P'_z and therefore to uncertainty in the dispersive bend angle. However, an uncertainty in the dispersive bend angle will induce uncertainties in both A_c and P'_z for $^2\mathrm{H}(\vec{e}, e'\vec{p})n$ that partially cancel one another, thus effectively reducing the contribution of the dispersive bend angle to the total systematic uncertainty on P'_z. In contrast, the analyzing power is relatively insensitive to P'_x and therefore to the uncertainty in the nondispersive bend angle and so no such compensation exists for P'_x. Therefore, the systematic uncertainty in P'_x receives contributions from both A_c and the nondispersive bend angle. The analyzing power cancels in P'_x/P'_z and so the systematic uncertainty on P'_x/P'_z receives contributions from both the dispersive and nondispersive bend angles.

VI. SUMMARY AND CONCLUSIONS

In conclusion, we measured the $^2\mathrm{H}(\vec{e}, e'\vec{p})n$ and $^1\mathrm{H}(\vec{e}, e'\vec{p})$ reactions at $Q^2 = 0.43$, 1.00, and 1.61 $(\mathrm{GeV}/c)^2$ for $p_m = 0$ and at $Q^2 = 1.00\ (\mathrm{GeV}/c)^2$ for p_m up to 170 MeV/c in Hall A of JLab. At low p_m, the longitudinal polarization, P'_z, exhibits a Q^2 dependence at variance with the reaction model for the deuteron. At high p_m, the same model fails to describe the transverse polarization, P'_x. These discrepancies indicate that nuclear effects in the $^2\mathrm{H}(\vec{e}, e'\vec{p})n$ reaction are not thoroughly understood and further study of this reaction is needed. The discrepancies also suggest that nuclear corrections in the related neutron electric form factor experiments need to be studied further.

ACKNOWLEDGMENTS

We acknowledge the outstanding support of the staff of the Accelerator and Physics Divisions at Jefferson Laboratory that made this experiment successful. We also acknowledge useful suggestions of R. Schiavilla. This work was supported in part by the U.S. Department of Energy contract DE-AC05-84ER40150 Modification No. M175 under which the Southeastern Universities Research Association operates the Thomas Jefferson National Accelerator Facility. We acknowledge additional grants from the U.S. DOE and NSF, the Italian INFN, the Canadian NSERC, and the Deutsche Forschungsgemeinschaft (SFB 443).

[1] I. Passchier *et al.*, Phys. Rev. Lett. **82**, 4988 (1999).
[2] G. Warren *et al.*, Phys. Rev. Lett. **92**, 042301 (2004).
[3] T. Eden *et al.*, Phys. Rev. C **50**, R1749 (1994).
[4] C. Herberg *et al.*, Eur. Phys. J. A **5**, 131 (1999).
[5] M. Ostrick *et al.*, Phys. Rev. Lett. **83**, 276 (1999).
[6] R. Madey *et al.*, Phys. Rev. Lett. **91**, 122002 (2003).
[7] D. I. Glazier *et al.*, Eur. Phys. J. A **24**, 101 (2005).
[8] A. I. Akhiezer and M. P. Rekalo, Sov. J. Part. Nuclei **4**, 277 (1974).
[9] R. G. Arnold, C. E. Carlson, and F. Gross, Phys. Rev. C **23**, 363 (1981).
[10] M. K. Jones *et al.*, Phys. Rev. Lett. **84**, 1398 (2000).
[11] O. Gayou *et al.* (Jefferson Lab Hall A Collaboration), Phys. Rev. Lett. **88**, 092301 (2002).
[12] V. Punjabi *et al.*, Phys. Rev. C **71**, 055202 (2005); **71**, 069902(E) (2005).
[13] S. Dieterich *et al.*, Phys. Lett. **B500**, 47 (2001).
[14] S. Strauch *et al.*, Phys. Rev. Lett. **91**, 052301 (2003).
[15] R. Ent, R. Ransome, S. Strauch, and P. E. Ulmer, JLab Experiment No. E03-104.
[16] A. Picklesimer and J. W. Van Orden, Phys. Rev. C **40**, 290 (1989).
[17] W. Fabian and H. Arenhövel, Nucl. Phys. **A314**, 253 (1979).
[18] H. Arenhövel, Phys. Lett. **B199**, 13 (1987).
[19] A. Yu. Korchin, Yu. P. Mel'nik, and A. V. Shebeko, Sov. J. Nucl. Phys. **48**, 243 (1988).
[20] M. P. Rekalo, G. I. Gakh, and A. P. Rekalo, J. Phys. G. **15**, 1223 (1989).

[21] J. M. Laget, Phys. Lett. **B273**, 367 (1990).
[22] B. Mosconi, J. Pauchenwein, and P. Ricci, in *Proceedings of the XIII European Conference on Few-Body Problems in Physics, 1991* (unpublished).
[23] H. Arenhövel (private communication).
[24] D. Eyl *et al*., Z. Phys. A **352**, 211 (1995).
[25] B. D. Milbrath *et al*., Phys. Rev. Lett. **80**, 452 (1998); **82**, 2221(E) (1999).
[26] J. Alcorn *et al*., Nucl. Instrum. Methods A **522**, 294 (2004).
[27] S. Dieterich, Ph.D. thesis, Rutgers University, 2002.
[28] E. L. Lomon, Phys. Rev. C **66**, 045501 (2002).
[29] O. Gayou *et al*., Phys. Rev. C **64**, 038202 (2001).
[30] R. Machleidt, K. Holinde, and Ch. Elster, Phys. Rep. **149**, 1 (1987).
[31] P. E. Ulmer, JLAB Technical Note No. 91–101, 1991.
[32] E. Borie and D. Drechsel, Nucl. Phys. **A167**, 369 (1971).
[33] P. G. Blunden, W. Melnitchouk, and J. A. Tjon, Phys. Rev. C **72**, 034612 (2005).
[34] B. Plaster *et al*., Phys. Rev. C **73**, 025205 (2006).
[35] K. Makino and M. Berz, Nucl. Instrum. Methods A **427**, 338 (1999).